Rotational Diffusion of Coumarins in Electrolyte Solutions: The Role of Ion Pairs

ARTICLE *in* THE JOURNAL OF PHYSICAL CHEMISTRY B · MARCH 2003

Impact Factor: 3.3 · DOI: 10.1021/jp027244l

2 AUTHORS:

GB Dutt
Bhabha Atomic Research Centre
75 PUBLICATIONS **1,626** CITATIONS
SEE PROFILE

Tapan Ghanty
129 PUBLICATIONS **2,173** CITATIONS
SEE PROFILE

Rotational Diffusion of Coumarins in Electrolyte Solutions: The Role of Ion Pairs

G. B. Dutt* and T. K. Ghanty

Radiation Chemistry & Chemical Dynamics Division, Bhabha Atomic Research Centre, Trombay, Mumbai 400 085, India

Received: October 18, 2002; In Final Form: January 17, 2003

In an attempt to explore how electrolyte ions influence the friction experienced by solutes with different functional groups, rotational diffusion of two structurally similar coumarins, coumarin 343 (C343) and coumarin 334 (C334), has been studied in dimethyl sulfoxide (DMSO) at several concentrations of $LiNO_3$. The two coumarins are almost identical except for the different functional groups in the 3-position; C343 has −COOH whereas C334 has $-COCH_3$. Because of the presence of the −COOH functional group, C343 exists as both anionic and neutral species in DMSO. Although both anionic and neutral forms of C343 exist in the ground state, C343 predominantly exists as neutral species in the excited state. The measured reorientation time of C343 in DMSO is slower by a factor of 2 compared to that of C334 due to the hydrogen bonding between the −COOH group of the probe and sulfoxide group of the solvent. However, the viscosity normalized reorientation times (τ_r/η) of C343 in $LiNO_3$/DMSO solutions increase by 60% to 70% compared to that in pure DMSO. Addition of electrolyte ions shifts the equilibrium toward the anionic form of C343, which in turn forms ion pairs with Li^+, and the large increase in τ_r/η values is due to the association of DMSO solvent molecules with these ion pairs. On the other hand, τ_r/η values of the neutral solute, C334, remain invariant in the entire range of the electrolyte concentration. The $C343^-Li^+$ ion pairs have been characterized using ab initio molecular orbital methods. Two approaches have been employed to model the friction experienced by the $C343^-Li^+$ ion pairs. In the first approach, the complex formed between $C343^-Li^+$ and the solvent molecules is treated as a rigid entity and the increase in the viscosity normalized reorientation time has been accounted for solely as an enhancement in the mechanical friction. Alternatively, the solvent association with the $C343^-Li^+$ ion pairs has been modeled as dielectric friction using the extended charge distribution theory.

1. Introduction

Solvent polarity and solute−solvent interactions are two of the most important factors that control the rates of chemical reactions in solution.[1] Hence considerable effort has gone into understanding these aspects in recent years. Among the many methods that are currently employed by researchers to examine the solute−solvent interactions, rotational diffusion studies are highly pragmatic. These studies have an added advantage over the others, as they enable us to solely explore the solute−solvent interactions due to the fact that the systems used are often nonreactive, thus eliminating the complications introduced by a chemical reaction.

A significant progress has been made toward understanding the solute−solvent interactions from the results of the rotational dynamics investigations.[2−44] Studies involving nonpolar solutes in nonpolar and/or polar solvents resulted in a wealth of information on how the friction experienced by the solute molecule depends on the macroscopic viscosity of the solvent, relative sizes of the solute and the solvent, and also on the free volume of the solvent.[3−12] On the other hand, studies with polar solutes in polar solvents has shed light on concepts such as dielectric friction[12−34] and solute−solvent hydrogen bonding[35−40] and how they cause additional friction on a rotating molecule.

More recently, rotational diffusion studies have been carried out in electrolyte solutions.[12,16,32,41−44] Although nonpolar, nondipolar, and polar solutes have been used in these investigations, studies involving ionic solutes resulted in very interesting observations. Hartman et al.[41] have measured the reorientation times of an anionic probe, resorufin in water and dimethyl sulfoxide (DMSO) at several concentrations of $LiNO_3$ in the range 0.0−2.0 M. Although they observed no change in the viscosity normalized reorientation times (τ_r/η) of resorufin in water with an increase in the electrolyte concentration, they found a 100% increase in the τ_r/η value of resorufin in DMSO from 0.0 to 2.0 M $LiNO_3$. Upon the addition of $LiNO_3$, resorufin anion forms ion pairs with Li^+ and the significant increase in τ_r/η has been rationalized as an enhancement in the mechanical friction due to the association of the solvent molecules with these ion pairs. In a latter study from the same group, Balabai and Waldeck[42] have reported the reorientation times of resorufin in DMSO in the presence of electrolytes KNO_3, $NaNO_3$, $LiNO_3$, and $Mg(NO_3)_2$ and could correlate the extent of ion pairing with the charge-to-size ratio of the cation. Further evidence for this ion pairing came from the molecular dynamics (MD) simulations by Balabai et al.[43] However, when similar studies were carried out with a trianion, methoxypyranine in DMSO with $LiNO_3$, they did not observe any increase in the τ_r/η value from 0.0 to 1.0 M electrolyte concentration.[44] From these studies, however, it is not obvious whether the phenomena of ion pairing in the presence of electrolytes and the subsequent increase in τ_r/η is universal to all organic anions or specific to resorufin. Also because the above-mentioned studies have been carried out in the ground state, it is not evident if a similar behavior will be observed in the excited state. The present study has been undertaken not only to address these issues but also to find out

* To whom correspondence should be addressed. E-mail: gbdutt@apsara.barc.ernet.in.

10.1021/jp027244l CCC: $25.00
Published on Web 03/14/2003

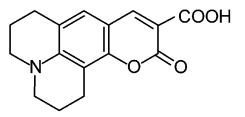

Coumarin 343

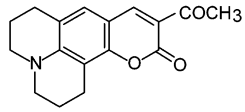

Coumarin 334

Figure 1. Molecular structures of the probes C343 and C334.

whether the solvent association with the ion pairs can be modeled as dielectric friction using the extended charge distribution theory. To meet these objectives, rotational diffusion of two structurally similar coumarins, coumarin 343 (C343) and coumarin 334 (C334), has been studied in DMSO at several concentrations of $LiNO_3$. The two coumarins used in the present study are almost identical except for the different functional groups in the 3-position; C343 has $-$COOH whereas C334 has $-COCH_3$ (see Figure 1 for the molecular structures of the probes). Because of the presence of the $-$COOH functional group, which is a weak acid, C343 exists both as anionic and neutral species in DMSO. It will be interesting to see whether C343 forms ion pairs with Li^+ analogous to resorufin or not. The remainder of the paper is organized in the following manner. Section 2 describes the experimental methods used to measure the reorientation times. Computational methods used to calculate the excited-state charge distribution of coumarins are discussed in section 3. Results are presented and analyzed in section 4, and the conclusions are summarized in the last section.

2. Experiment

The probes C343 and C334 are of the highest available purity from Exciton. Spectroscopy grade DMSO is from Sisco Research Laboratories Private Ltd., India. Both the probes and the solvent were used without further purification. $LiNO_3$ is from Aldrich Chemicals and was dried for 8 h in a vacuum oven at 333 K. In all the measurements, the concentration of the coumarins was kept in the range $10^{-5}-10^{-6}$ M.

Absorption spectra were recorded using JASCO V-530 spectrophotometer, and the emission spectra, using Hitachi F-4010 spectrofluorometer. Time-resolved fluorescence depolarization method was employed to measure the reorientation times. The experiments were carried out using the time-correlated single-photon counting[45] facility at the Tata Institute of Fundamental Research, Mumbai. The excitation source is a picosecond frequency-doubled Ti:saphire laser (Tsunami, Spectra Physics), and the details have been described elsewhere.[38] Both the coumarins were excited at 440 nm with a vertically polarized pulse and the fluorescence decays were collected at 500 nm by keeping the emission polarizer parallel $I_{||}(t)$, perpendicular $I_{\perp}(t)$, and also at the magic angle $I(t)$ (54.7°) with respect to the excitation polarization. For the parallel component of the decay, 10 000 peak counts were collected and the perpendicular component of the decay was corrected for the polarization bias of the detection system, the *G*-factor. The decays were collected in 512 channels of a multichannel analyzer with a time increment of 42.7 ps/channel. The measured decays were convoluted with the instrument response function, which was measured by a sample that scatters light. All the measurements were carried out at 298 K and the temperature was maintained within ±1° with the help of a temperature controller, Eurotherm. From the measured anisotropy decays, the parameters were obtained by a simultaneous fit of both the parallel and the perpendicular decay components with the help of a nonlinear least-squares routine that uses the Marquardt algorithm as described by Bevington.[46,47] The parameters, fluorescence lifetime τ_f, rotational reorientation time τ_r, and the limiting anisotropy r_0 were held common for both the decays during the analysis. The goodness of the fit was judged from the statistical parameters such as the reduced χ^2 being close to unity, random distribution of the weighted residuals, etc. Each measurement was repeated 2−3 times and the analysis was performed from the peak of $I_{||}(t)$ as well as 150 ps before the peak and the average value is reported.

3. Computational Methods

Ab initio molecular orbital methods were used to determine the structure and charge distributions of the C343 as well as the C334 molecules. The ground-state global minimum geometries of both the species were fully optimized (without any symmetry constraint) at the Hartree−Fock level of theory with a 6-31G** basis set. With this basis set the total number of orbitals generated are 390 and 400 for C343 and C334, respectively (with 75 occupied orbitals in both the cases). Using the ground-state optimized geometries, vertically excited singlet-state calculations were performed using configuration interaction method with single and double excitations (SDCI). However, with the present day computer resources it is not possible to correlate all the valence electrons in the full valence CI space for molecules such as C343 or C334. In view of this, we have limited the CI calculations by taking 40 valence electrons and 40 orbitals for both C343 and C334, which resulted in 80 601 configurations for each molecule. Hartree−Fock orbitals have been used to perform SDCI calculations. The geometry of the ion-paired species containing the $C343^-$ anion and Li^+ cation was also optimized using the same basis set and at the same level of theory. The excited-state calculation for the ion pair species was performed in the same manner, as was done for the C343 and C334 molecules. For all the species, partial atomic charges for the excited singlet state were calculated using Mulliken population analysis scheme. The geometry of the solvent associated ion-paired species with two DMSO molecules was optimized using STO-3G basis set, which is consistent with the literature reports of the coordination number for these cations in DMSO.[48] All the calculations in this work were done using the GAMESS[49] electronic structure program.

4. Results and Discussion

Figure 2 gives absorption and emission spectra of C343 in DMSO under different conditions. In DMSO, C343 exists both as neutral and anionic species. The absorption maxima at 438 nm corresponds to the neutral form of C343. In the presence of a weak base like $NaHCO_3$ (10^{-3} M), the equilibrium shifts toward the anionic form, which has a peak at 395 nm. Upon the addition of 0.1 and 2.0 M $LiNO_3$, the absorption maxima of C343 in DMSO shifts to 423 and 430 nm, respectively. The presence or absence of 10^{-3} M $NaHCO_3$ has no effect on the spectra of C343 when $LiNO_3$ is added. Addition of electrolyte favors the formation of ion-paired species between the $C343^-$ anion and Li^+ cation. However, such pronounced changes are not observed in the case of the emission spectra. The emission spectra of C343 in DMSO and in the presence of 2.0 M $LiNO_3$ has the same peak position, at 484 nm. At low salt concentration (0.1 M $LiNO_3$), the peak position is blue shifted by about 7 nm. The emission spectra of the C343 anion has a maxima at 503 nm. In the case of C334, however, both the absorption and

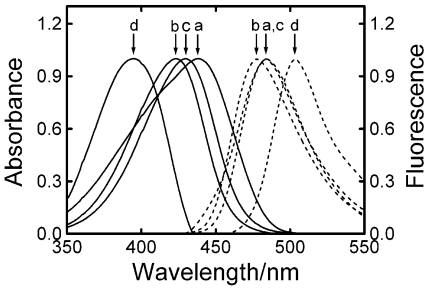

Figure 2. Absorption (solid line) and emission (dashed-line) spectra of C343 in DMSO: (a) 0.0 M $LiNO_3$; (b) 0.1 M $LiNO_3$; (c) 2.0 M $LiNO_3$; (d) 10^{-3} M $NaHCO_3$. In DMSO, C343 exists in two forms, neutral as well as anionic (a). In presence of electrolyte, it exists predominantly as ion-paired species (b, c). Addition of a weak base shifts the equilibrium and favors the anionic form (d). In the excited state, however, neutral and ion-paired forms are more stable (see text for details).

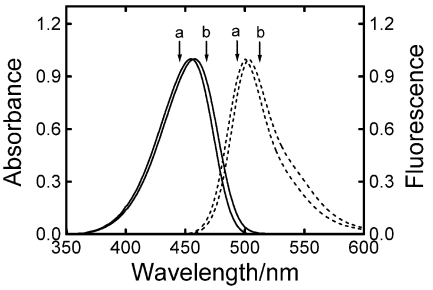

Figure 3. Absorption (solid line) and emission (dashed-line) spectra of C334 in DMSO: (a) 0.0 M $LiNO_3$; (b) 2.0 M $LiNO_3$. No appreciable changes in the absorption and emission spectra are observed upon the addition of electrolyte. Both the absorption and emission spectra are red-shifted by a few nanometers in the presence of the electrolyte.

emission maxima upon the addition of 2.0 M $LiNO_3$ are red shifted by 3 nm compared to that in DMSO (see Figure 3).

The fluorescence decay of C343 in DMSO exhibits biexponential behavior in the absence of any additives. Although both neutral and anionic species are present in the ground state, in the absence of electrolyte, C343 predominantly exists as neutral species in the excited state. This has been reflected in the preexponential factors obtained from the analysis of the fluorescence decay. The lifetimes of neutral and anionic forms are 3.52 ns and 1.60 ns, respectively, and the corresponding preexponential factors are 95% and 5%. Excitation of the anionic form of C343 (in the presence of 10^{-3} M $NaHCO_3$) at 395 nm resulted in a slight increase of the anionic component from 5% to 15%. To shift the equilibrium completely toward the anionic form, either high concentration of weak base or low concentration of strong base is needed.[50,51] The required alkaline environment may alter the viscous and dielectric properties of the solvent significantly. Moreover, it has been found that C343 decomposed rapidly in strong alkaline solutions.[50] In view of these difficulties, all the experiments have been carried out without the addition of alkali. However, in the presence of $LiNO_3$, it appears that the equilibrium is shifted toward the anionic form of C343, which is stabilized by the formation of ion pairs with Li^+ and as a consequence the fluorescence of C343 decays with only one lifetime. Indirect evidence for such a hypothesis will be presented later during the course of the discussion. The fluorescence lifetimes of C343 in DMSO almost remain the same (3.50 ns) with an increase in $LiNO_3$ concentration from 0.1 to 2.0 M. On the other hand, the fluorescence decay of C334 in DMSO from 0.0 to 2.0 M $LiNO_3$ exhibits single-exponential behavior with a lifetime of 3.20 ns and there is no change in this lifetime with an increase in the electrolyte concentration.

TABLE 1: Rotational Reorientation Times (τ_r) of C343 and C334 in DMSO as a Function $LiNO_3$ Concentration, Together with Viscous and Dielectric Properties of the Electrolyte Solutions

				τ_r/ps	
$[LiNO_3]$/M	η/mPa s[a]	ϵ_0[b]	τ_D/ps[b]	C343	C334
0.00	1.98	47.3	19.6	233 ± 27	123 ± 2
0.10	2.10	46.0	19.9	365 ± 25	136 ± 7
0.25	2.37	44.3	20.5	449 ± 28	156 ± 10
0.50	2.89	41.5	22.2	573 ± 17	183 ± 9
0.75	3.54	39.6	24.3	711 ± 26	227 ± 34
1.00	4.35	38.0	27.0	870 ± 29	272 ± 26
1.25	5.38	36.3	30.6	1065 ± 60	342 ± 23
1.50	6.65	35.2	34.7	1285 ± 34	416 ± 17
2.00	10.30	34.0	45.0	1941 ± 60	657 ± 31

[a] Viscosity data from ref 41. [b] Dielectric parameters interpolated from ref 68.

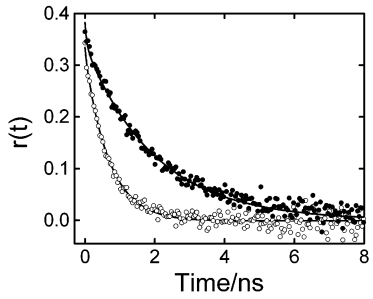

Figure 4. Anisotropy decays of C343 (filled circles) and C334 (open circles) in DMSO + 2.0 M $LiNO_3$. The smooth lines through the experimental data points are the fitted ones.

The anisotropy decays of both C343 and C334 in DMSO at all concentrations of $LiNO_3$ are adequately described by single exponential functions. Even in the case of C343 in DMSO, where the fluorescence decay is biexponential, only one reorientation time is obtained. This is because the two reorientation times are not significantly different from one another. To obtain biexponential anisotropy decay, the two reorientation times should differ at the least by a factor of 5 or more. Otherwise, the recovered τ_r represents the average of the two reorientation times. In the case of C343 in DMSO, however, the decay of anisotropy has very little contribution from the anionic form because it predominantly exists as neutral species. The reorientation times of C343 and C334 at several concentrations of $LiNO_3$ in DMSO are given in Table 1. The viscous and dielectric properties of $LiNO_3$/DMSO solutions are also given in the table. It can be seen from the table that in DMSO the reorientation time of C343 is nearly 2 times slower than that of C334, but in the presence of $LiNO_3$ this ratio ($\tau_r^{C343}/\tau_r^{C334}$) is around 3. Figure 4 gives the anisotropy decays of C343 and C334 in DMSO with 2.0 M $LiNO_3$. It is visually obvious from the figure that C343 rotates significantly slower than C334. Another observation is that the τ_r values of both C343 and C334 increase by a factor of 8.3 and 5.3, respectively, from 0.0 to 2.0 M $LiNO_3$. This is not surprising because the viscosity of DMSO increases by a factor of 5.2 upon the addition of 2.0 M $LiNO_3$. To get a better appreciation of these differences, the viscosity normalized reorientation times of C343 and C334 are plotted as a function of $LiNO_3$ concentration in Figure 5. The τ_r/η value of C343 at 0.1 M $LiNO_3$ increases by 47% compared to that in DMSO. At higher concentrations of $LiNO_3$ this increase is in the range of 60% to 70%. In fact from 0.25 to 2.0 M $LiNO_3$, τ_r/η fluctuates around an average value of 195 ± 6

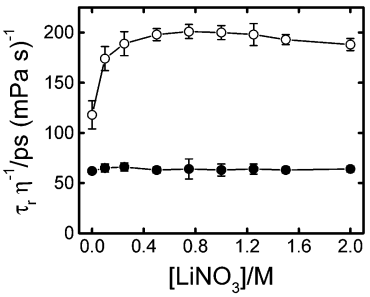

Figure 5. Viscosity normalized reorientation times of C343 (open circles) and C334 (filled circles) as a function of $LiNO_3$ concentration. The lines through the experimental points are drawn as a visual aid. In the case of C334, the reorientation times correlate well with the solution viscosity.

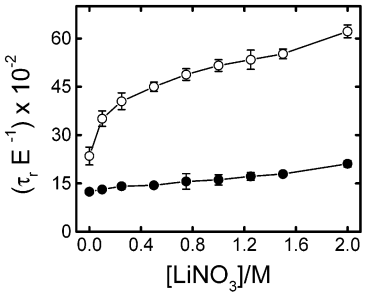

Figure 6. Reorientation times of C343 (open circles) and C334 (filled circles) normalized by the dielectric parameter, $E = (\epsilon_0 - 1)/(2\epsilon_0 + 1)^{-2}\tau_D$, as a function of $LiNO_3$ concentration. The lines through the experimental points are drawn as a visual aid. In the case of C334, the reorientation times correlate reasonably well with the solution dielectric parameters.

ps (mPa s)$^{-1}$. In contrast, τ_r/η values of C334 remain invariant with an increase in the electrolyte concentration. Addition of $LiNO_3$ to DMSO also alters the dielectric constant ϵ_0 and Debye relaxation time τ_D of the solution (see Table 1). The reorientation times of C343 and C334 normalized with the dielectric parameter $E = (\epsilon_0 - 1)(2\epsilon_0 + 1)^{-2}\tau_D$ are plotted as a function of [$LiNO_3$] in Figure 6. The reorientation times of C343 normalized with the dielectric parameter increase significantly with $LiNO_3$ concentration. On the other hand, those of C334 correlate reasonably well with the dielectric parameter. These results will be analyzed within the framework of hydrodynamic, dielectric friction theories and also using the concept of ion pairing in the case of C343 in $LiNO_3$/DMSO solutions.

A. Mechanical Friction. In the absence of other frictional forces that hinder the molecular rotation in liquids, the reorientation time is proportional to the solvent viscosity η and the volume of the solute V. According to the Stokes−Einstein−Debye hydrodynamic theory,[52] the reorientation time is given by

$$\tau_r = \frac{\eta V}{kT}(fC) \tag{1}$$

where f is the shape factor introduced by Perrin[53] to account for the nonspherical shape of the solute and C is the boundary condition that determines the extent of coupling between the solute and the solvent.[2] k and T are the Boltzmann constant and absolute temperature, respectively.

To calculate the mechanical friction experienced by C343 and C334, the axial radii of both the probes were measured from Corey−Pauling−Koltum (CPK) scaled atomic models and are given in Table 2. The van der Waals volumes that were calculated using the Edwards increment method[54] are also given in the table. Both the probes were treated as asymmetric ellipsoids and the friction coefficients (ζ_i's) along the three principal axes of rotation with slip and stick boundary conditions were obtained by interpolating the numerical tabulations.[55,56] From these friction coefficients, the corresponding diffusion coefficients (D_i's) were obtained using the Einstein relation[57]

TABLE 2: Properties of the Solutes

					$\tau_r\eta^{-1}$/ps (mPa s)$^{-1}$	
solute	axial radii/Å^3	V/Å^3	f	C_{slip}	slip	stick
Coumarin 343	6.6 × 4.5 × 1.9	243	1.99	0.18	21	118
Coumarin 334	7.0 × 4.5 × 1.9	252	2.10	0.22	28	129
Coumarin 153[a]	6.1 × 4.8 × 2.0	246	1.67	0.14	14	100

[a] From ref 26.

$$D_i = \frac{kT}{\zeta_i} \tag{2}$$

The reorientation time was obtained from the diffusion coefficients using the relation[22]

$$\tau_r = \frac{1}{12}\left[\frac{4D_x + D_y + D_z}{D_xD_y + D_yD_z + D_zD_x}\right] \tag{3}$$

This equation is derived under the assumption that the transition dipole is along the long axis of the molecule. The reorientation times at unit viscosity calculated with slip and stick boundary conditions together with the shape factor and C_{slip} are given in Table 2. Inspection of the table reveals that for a 6% change in the long axial radius between C343 and C334, the reorientation time at unit viscosity calculated with slip boundary condition varies by 33%. However, the variation in τ_r/η calculated using the stick boundary condition is only 9%. Because C343 and C334 are similar in shape and size, they are expected to experience identical mechanical friction for a particular boundary condition. But in practice, the theoretically calculated τ_r/η values with slip boundary condition for the two coumarins are quite different. To see how these τ_r/η values compare with that of another structurally similar probe, the properties of coumarin 153 (C153), taken from ref 26 are also given in the table. C153 is almost similar to C343 and C334 except that it has a $-CF_3$ functional group in the 4-position instead of the −COR group in the 3-position. Its long axial radius is shorter by 15% and the short-in-plane radius is longer by 7% compared to that of C334. However, the reorientation time calculated with slip boundary condition is 100% smaller than that of C334, whereas the one obtained with stick boundary condition is smaller by only 29%. This exercise once again confirms that the calculated τ_r/η values with slip boundary condition are indeed extremely sensitive to minor changes in the axial radii. What is the reason for the large variation in the calculated reorientation times, especially in the case of slip boundary condition, with subtle changes in the axial radii? The reason being, with slip boundary condition only motions that displace the solvent molecules give rise to any friction and hence the calculated τ_r values strongly depend on the axial ratio. Under these circumstances, what is the best possible way to obtain an estimate on the mechanical friction experienced by these coumarins? One of the methods that has often been employed, though not necessarily correct, is to measure the reorientation times in nonpolar solvents because the friction experienced by the probes in these solvents is purely mechanical. Horng et al.[26] have measured the reorientation times of C153 in a number of nonpolar solvents of different sizes in the viscosity range of 0.29 to 28.4 mPa s

and obtained an empirical relation of the form

$$\tau_r = 34.8\eta^{0.63} \quad (4)$$

Because C343 and C334 are similar to C153 in size and shape, eq 4 can be used to obtain the mechanical friction experienced by these probes in DMSO. However, this kind of empirical relation does not take into consideration parameters such as the size and free volume of the solvent. It has been hypothesized theoretically[58,59] and proven experimentally[3−10,26,29] that the friction experienced by the probe is indeed sensitive to both these parameters of the solvent. In view of these limitations, it is more appropriate to choose a solvent whose size and free volume are closer to that of DMSO. Inspection of Table 1 in ref 26 reveals that *n*-hexane is the closest to DMSO in size even though it is bigger than DMSO by about 50%. However, the free volumes, calculated from the Hilderbrand−Batschinski parameter and isothermal compressibility values given in refs 7 and 21, are identical (40 Å^3) for both *n*-hexane and DMSO at 298 K. Hence, it is fairly reasonable to use the measured reorientation time of C153 in *n*-hexane to obtain the mechanical friction experienced by C343 and C334 in DMSO. The τ_r/η value obtained from the measured reorientation time of C153 in *n*-hexane is 45 ps (mPa s)$^{-1}$. From this number the hydrodynamic component of the reorientation time for the probes C343 and C334 in DMSO was obtained, which is 89 ps. The mechanical friction calculated in this manner accounts for only 38% of the total friction experienced by C343 in DMSO, and in the case of C334 this number is 72%.

B. Dielectric Friction. Dielectric friction is one of the important mechanisms that hinders the rotation of the polar molecules in polar solvents. The response of the solvent polarization that is induced by the solute's dipole or its charge distribution is slow compared to the rotation of the solute. Hence it acts as an additional drag on the rotating molecule and is known as the dielectric friction. Among the continuum theories of dielectric friction, point dipole models of Nee−Zwanzig (NZ)[60] and van der Zwan−Hynes (ZH)[61] are often used by the experimentalists.[12−20,26−29,34] However, more recent studies[20−25,30−33,41−44] have employed the extended charge distribution model of Alavi−Waldeck (AW).[62,63] In this theory, it is the charge distribution of the solute rather than the dipole moment that is used to calculate the friction experienced by the solute molecule. According to this model, not only the dipole moment of the solute but also the higher order moments contribute significantly to the dielectric friction. In other words, molecules having no net dipole moment can also experience dielectric friction. It has been found that the AW theory is successful compared to NZ and ZH theories in modeling the friction experienced by the solutes in nonassociative solvents.[20−25,30−32] The expression for the dielectric friction according to the AW model is given by[63]

$$\zeta_{DF} = \frac{8}{a}\frac{(\epsilon_0 - 1)}{(2\epsilon_0 + 1)^2}\tau_D \sum_{j=1}^{N}\sum_{i=1}^{N}\sum_{L=1}^{L_{max}}\sum_{M=1}^{L}\left(\frac{2L+1}{L+1}\right)\frac{(L-M)!}{(L+M)!} \times M^2 q_i q_j \left(\frac{r_i}{a}\right)^L \left(\frac{r_j}{a}\right)^L P_L^M(\cos\theta_i) P_L^M(\cos\theta_j) \cos M\phi_{ji} \quad (5)$$

where $P_L^M(x)$ are the associated Legendre polynomials, a is the cavity radius, N is the number of partial charges, q_i is the partial charge on atom i, whose position is given by (r_i,θ_i,ϕ_i), and $\phi_{ji} = \phi_j - \phi_i$. Although the AW theory also treats the solvent as a structure less continuum like the NZ and ZH theories, it provides a more realistic description of the electronic properties of the solute.

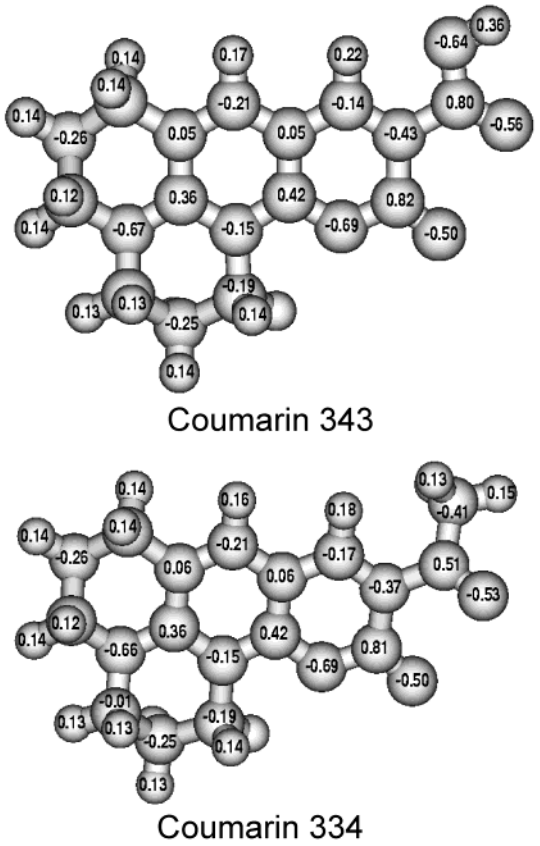

Figure 7. Partial atomic charge distributions of C343 and C334 in the excited state.

To calculate the friction experienced by the solute molecule using this model, the value of L_{max} and the cavity radius must be known besides the charge distribution of the solute and the dielectric properties of the solvent. The excited-state charge distribution of coumarins was obtained as described in section 3, and they are presented in Figure 7. L_{max} is the cutoff value of L above which the solvent cannot respond to the spatial variation in the charge distribution of the solute. In solvents such as DMSO, which is nonassociative, the value of L_{max} can be chosen by computing the number of solvent molecules that can be packed on the surface of the cavity. Hence, the value of L_{max} depends on the relative size of the solute and the solvent and can be calculated using the formula[22]

$$L_{max} = 2\frac{(r_{solute} + r_{solvent})^2}{(r_{solvent})^2} \quad (6)$$

where r_{solute} and $r_{solvent}$ are the radii of the solute and the solvent, respectively. The respective long axial radii were taken as r_{solute} for C343 and C334 and $r_{solvent}$ for DMSO was obtained from the van der Waals volume of the solvent and treating it as a sphere, which is 2.64 Å. The L_{max} values obtained for C343/DMSO and C334/DMSO using eq 6 are 25 and 27, respectively. The friction calculated using the AW model is extremely sensitive to choice of the cavity radius because the charges are closer to the cavity boundary. In view of this limitation, the value of the cavity radius is used as an adjustable parameter. However, the best-fit cavity radius should be realistic and closer to the long axial radius of the solute molecule. Equation 5 was used to calculate the dielectric friction experienced by C343

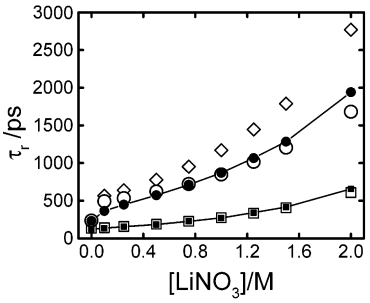

Figure 8. Plots of the experimentally measured reorientation times of C343 (filled circles) and C334 (filled squares) as a function of $LiNO_3$ concentration. The lines through the experimental points are drawn as a visual aid. The open squares represent the calculated reorientation times for C334 using the combination of mechanical and dielectric frictions. The open diamonds represent mechanical friction calculated for the solvent associated $C343^-Li^+$ ion pairs with stick boundary condition. The open circles represent the calculated reorientation times for C343 and $C343^-Li^+$ ion pairs using the combination of mechanical and dielectric frictions (see text for details).

and C334 in DMSO. The dielectric friction coefficients along the three principal axes were computed by redefining the angles θ and ϕ with respect to each axis. The total friction about each axis was obtained by summing the mechanical and dielectric friction contributions using the relation

$$\zeta_{\text{total}} = \zeta_{\text{mech}} + \zeta_{\text{DF}} \tag{7}$$

However, the decomposition of total friction into mechanical and dielectric components is not correct conceptually[44,64,65] but acts as a useful approximation while the total friction is calculated from the mechanical and dielectric components. From ζ_{total} along each axis, the diffusion coefficients were calculated using eq 2 and the reorientation times were obtained from the D_i values using eq 3.

The best-fit cavity radius for C334/DMSO at different concentrations of $LiNO_3$ is 7.53 Å. The agreement between the experimentally measured reorientation times and the theoretically calculated numbers is within 10%. The value of the best-fit cavity radius is about 8% longer than the long axial radius of C334. Figure 8 gives plots of τ_r vs [$LiNO_3$] for C334 in DMSO and the theoretically calculated numbers are also given in the figure. As mentioned earlier, in the case of C343/DMSO, the reorientation time is about 2 times slower compared to that of C334 because of the hydrogen bonding interactions between the carboxylic group of C343 and the sulfoxide group of the solvent. The specific interactions can also be modeled as dielectric friction using the extended charge distribution theory because both dielectric friction and hydrogen bonding interactions are electrostatic in nature. The practice of modeling specific interactions as dielectric friction has been adopted in the literature recently.[32−34] In our recent work[32] involving the nondipolar probe, 1,4-dioxo-3,6-diphenylpyrrolo[3,4-*c*]pyrrole (DPP), we have shown that the specific interactions between the secondary amino groups of the probe and DMSO can be modeled as dielectric friction using the AW model. The best-fit cavity radius for C343/DMSO is 7.22 Å and is 9% longer than the long axial radius of C343. The best-fit cavity radius obtained for C343 is about 4% smaller than that obtained for C334, which is in qualitative accord with the long axial radii of these solute molecules. However, in the presence of $LiNO_3$, the same charge distribution and the cavity radius (7.22 Å) that was used for C343 could only reproduce numbers that are 50% to 100% smaller than the experimentally measured values, which indicates that the friction experienced by $C343^-Li^+$ ion pairs is of a different nature compared to the one experienced by C343.

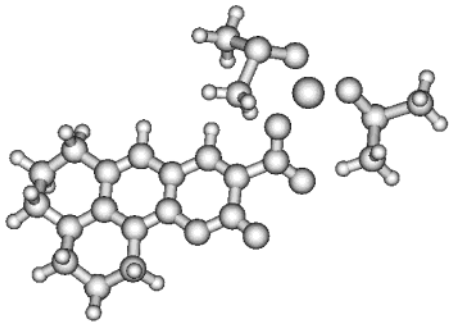

Figure 9. One of the possible structures of the $C343^-Li^+$ ion-paired species associated with two DMSO molecules optimized using STO-3G basis set.

C. Friction Due to Ion Pairing. The significant increase in the viscosity normalized reorientation times of C343 in the presence of $LiNO_3$/DMSO can be attributed to ion pairs of the form $C343^-Li^+$ and these ion pairs in turn associate with the solvent molecules. A similar pattern has been observed for another anionic probe, resorufin in electrolyte solutions of DMSO and methanol by Waldeck and co-workers.[41−44]

Alternatively, it may also be possible to argue that the neutral form of C343 itself is associating with DMSO solvent molecules instead of $C343^-Li^+$ ion pairs, as there is no variation in the τ_r/η values with electrolyte concentration except at 0.1 M $LiNO_3$. If that is the situation, then the τ_r/η values of C343 should have decreased instead of increasing in the presence of electrolyte compared to that in neat DMSO, which is due the fact that the electrolyte ions shield the hydrogen bonding sites between the solute and the solvent. In other words, electrolyte ions do not facilitate the formation of solute−solvent hydrogen bonding and as a consequence τ_r/η values decrease with an increase in the electrolyte concentration. In fact, this kind of decrease in τ_r/η values has been observed for positively charged hydrogen bonding solutes such as cresyl violet and thionine, both possessing amino groups[43] and also for nondipolar solute DPP that has two secondary amino groups[32] in electrolyte solutions of DMSO. In view of the arguments presented here, we have used the association between the $C343^-Li^+$ ion pairs and DMSO rather than C343/DMSO to comprehend the observed results. Now the question that needs to be addressed is, what is the nature of the friction experienced by these ion pairs? Is it mechanical friction or dielectric friction or a combination of both? Hartman et al.[41] have treated the friction experienced by resorufin$^-Li^+$ ion pairs as an enhancement in the mechanical friction due to the solvent association in their analysis. Also from the analysis of resorufin$^-Li^+$ and resorufin$^-Na^+$ ion pairs in DMSO, Balabai and Waldeck[42] found that the dielectric friction experienced by these ion pairs is not significant compared to the mechanical friction. In our analysis, however, the additional friction experienced by $C343^-Li^+$ ion pairs will be treated solely as an enhancement in the mechanical friction due to the association of the solvent molecules, and alternatively, the solvent association with the ion pairs will be treated as dielectric friction using the extended charge distribution theory.

Each $C343^-Li^+$ ion pair can associate with two molecules of DMSO[48] and can form a rigid complex, as shown in Figure 9. The axial radii of the solvent associated $C343^-Li^+$ ion pairs are $9.8 \times 5.1 \times 1.9$ Å^3, and they have a van der Waals volume of 395 Å^3. The ion-paired solvent complex was treated as an asymmetric ellipsoid, and the viscosity normalized reorientation

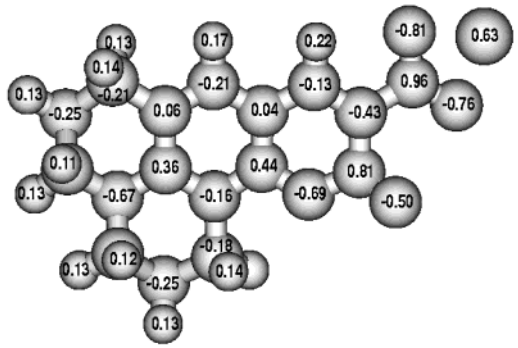

Figure 10. Partial atomic charge distribution of $C343^{-}Li^{+}$ ion pair in the excited state.

times that were calculated with slip and stick boundary conditions are 87 ps (mPa s)$^{-1}$ and 269 ps (mPa s)$^{-1}$, respectively. As the size of the solute molecule increases compared to the solvent molecule, the mechanical friction experienced by the solute should approach the stick limit, which has been proven experimentally by quite a few studies in the literature.[5,7,9] From their experimental measurements and by compiling the data from literature, Roy and Doraiswamy[7] found that the ratio of the measured reorientation time to the calculated one with stick boundary condition (τ_r/τ_{stick}) increases from 0.06 to 0.85 as the volume of the solute goes up from 66 Å^3 to 733 Å^3. The τ_r/τ_{stick} values obtained for $C343^{-}Li^{+}$ ion pairs are around 0.70, and this number is consistent with the values reported in the literature for solute molecules whose volumes are around 400 Å^3. Experimentally measured and theoretically calculated reorientation times of $C343^{-}Li^{+}$ ion pairs as a function of [$LiNO_3$] are shown in Figure 8 for comparison.

An equally plausible, but mechanistically different, approach is to model the additional friction experienced by the ion pairs as dielectric friction. Figure 10 gives the excited-state charge distribution of $C343^{-}Li^{+}$ ion pairs. The excited-state charge distributions of C343 and $C343^{-}Li^{+}$, especially the charges on the hydrogen atom and the Li^{+} ion, are significantly different (see Figure 7 and Figure 10 for comparison). Because the charge distributions of C343 and $C343^{-}Li^{+}$ are dissimilar, their interaction with DMSO will be different and hence the contribution of the dielectric friction. However, because both C343 and $C343^{-}Li^{+}$ are similar in size and shape, the mechanical friction experienced by $C343^{-}Li^{+}$ will be identical to that of C343. Employing the same values for the mechanical friction that were used for C343, the dielectric friction experienced by $C343^{-}Li^{+}$ ion pairs was calculated using the AW theory and the reorientation time with eq 3 as described before. The best-fit cavity radius for $C343^{-}Li^{+}$ ion pair was found to be 7.94 Å, which is 10% longer than that obtained for C343. This is not surprising considering the fact that the ionic radius of Li^{+} (0.74 Å)[42] is larger than the covalent radius of the hydrogen atom (0.3 Å).[66] The agreement between the experimentally measured values and theoretically calculated (sum of mechanical and dielectric friction components) numbers is within 20%, and they are plotted in Figure 8.

D. Limitations in the Modeling. Even though the friction experienced by the $C343^{-}Li^{+}$ ion pairs has been modeled as an enhancement in the mechanical friction using the pictorial depiction in Figure 9, this kind of modeling is not rigorous because it is an oversimplification of the real situation. According to Balabai and Waldeck[42] the electrolyte solution will have a distribution of ion pairs with different geometries and the picture given in Figure 9 represents one of the possible ion-paired species. Also it is very difficult to predict the shape of the solvent associated ion pairs accurately. In view of these limitations, the modeling done here only illustrates the fact that ion-pairing plays a significant role in the friction experienced by charged solute molecules.

Similar studies[41−43] from Waldeck's group with the probe resorufin in $LiNO_3$/DMSO solutions proved the existence of free resorufin and ion-paired resorufin in equilibrium with each other and the respective mole fractions were found to be dependent on the concentration of the electrolyte. The τ_r/η values of resorufin were found to increase gradually with [$LiNO_3$] and reach a saturation value. They could also estimate the mole fractions of free and ion-paired species using conductivity measurements. However, in our study, we have assumed that in the presence of $LiNO_3$, C343 predominantly exists as ion-paired species because as mentioned earlier, the τ_r/η values from 0.25 to 2.0 M $LiNO_3$ fluctuate around an average value of 195 $\pm$ 6 ps (mPa s)$^{-1}$. Only at 0.1 M $LiNO_3$, is the τ_r/η value 174 $\pm$ 12 ps (mPa s)$^{-1}$, which is about 12% smaller than the average value and it may be possible that both neutral and ion-paired forms of C343 are in equilibrium at this concentration. Unlike the studies from Waldeck's group, our experiments have been carried out in the excited state and hence conductivity measurements cannot be employed to obtain the mole fractions of neutral and ion-paired forms of C343, even if they exist in equilibrium.

Modeling the friction experienced by the $C343^{-}Li^{+}$ ion pairs as dielectric friction using the AW extended charge distribution theory, however, appears to be more realistic because the charge distribution of the ion pairs could be calculated fairly accurately using ab initio molecular orbital methods. But one serious limitation in applying the AW theory is the choice of the cavity radius because the friction calculated using this theory is extremely sensitive to the subtle variations in the values of the cavity radius. The probable reasons for this could be that the charges are closer to the cavity boundary and also the AW model does not explicitly include the structural features of the solvent. However, the best-fit cavity radii appear to be realistic considering the fact that the *a* value obtained for the $C343^{-}Li^{+}$ ion pair is larger than that obtained for C343.

Because the present study has been carried out in electrolyte solutions, another issue that needs to be addressed is the contribution of the ion atmosphere friction to the total friction. The ion atmosphere arises from the nonuniform distribution of charged species in solution, which creates an additional mechanism for friction, known as ion atmosphere friction. This type of friction is caused by the finite response time of the ion atmosphere about the solute, which generates a torque that opposes the probe molecule's rotation and increases friction. However, it has been found from experimental studies that the contribution due to ion atmosphere friction is only about 3% of the total friction experienced by the solute molecules.[67]

5. Conclusions

Rotational diffusion of two structurally similar coumarins, C343 and C334, has been investigated in DMSO at several concentrations of $LiNO_3$ with an intent to find answers to the following queries. How is the friction experienced by solutes with different functional groups affected in the presence of electrolyte ions? What is the nature of the friction experienced by ion pairs? Is it simply enhanced mechanical friction due to solvent association or whether the ion pair/solvent association can be modeled as dielectric friction? The important conclusions from the study are as follows. The viscosity normalized reorientation times of C343 increase significantly in $LiNO_3$/DMSO solutions compared to that in pure DMSO, whereas those

of C334 remain the same. This increase in τ_r/η values of C343 in the presence of $LiNO_3$ is due to the formation of $C343^-Li^+$ ion pairs, which in turn associate with DMSO solvent molecules. The significant increase in the viscosity normalized reorientation times has been interpreted as an enhancement in the mechanical friction of the solvent associated $C343^-Li^+$ ion pairs compared to that of C343. Alternatively, the increase in τ_r/η has also been interpreted as dielectric friction experienced by the $C343^-Li^+$ ion pairs using extended charge distribution theory of Alavi−Waldeck. However, it must be emphasized that the models used here to account for the friction experienced by the ion pairs are justified within some limitations.

Acknowledgment. We are grateful to Dr. Ira for her help with the time-resolved fluorescence measurements. We thank Mr. G. Rama Krishna for useful discussions. We also thank Drs. A. V. Sapre, S. K. Ghosh, T. Mukherjee, and J. P. Mittal for their encouragement throughout the course of this work.

References and Notes

(1) Reichardt, C. *Solvents and Solvent Effects in Organic Chemistry*, 2nd ed.; VCH: New York, 1988.
(2) Fleming, G. R. *Chemical Applications of Ultrafast Spectroscopy*; Oxford University Press: New York, 1986.
(3) Courtney, S. H.; Kim, S. K.; Canonica, S.; Fleming, G. R. *J. Chem. Soc., Faraday Trans. 2* **1986**, *82*, 2065.
(4) Ben-Amotz, D.; Scott, T. W. *J. Chem. Phys.* **1987**, *87*, 3739.
(5) Ben-Amotz, D.; Drake, J. M. *J. Chem. Phys.* **1988**, *89*, 1019.
(6) Kim, S. K.; Fleming, G. R. *J. Phys. Chem.* **1988**, *92*, 2168.
(7) Roy, M.; Doraiswamy, S. *J. Chem. Phys.* **1993**, *98*, 3213.
(8) Anderton, R. M.; Kauffman, J. F. *J. Phys. Chem.* **1994**, *98*, 12117.
(9) S. De Backer, S.; Dutt, G. B.; Ameloot, M.; De Schryver, F. C.; Müllen, K.; Holtrup, F. *J. Phys. Chem.* **1996**, *100*, 512.
(10) Benzler, J.; Luther, K. *Chem. Phys. Lett.* **1997**, *279*, 333.
(11) Jas, G. S.; Wang, Y.; Pauls, S. W.; Johnson, C. K.; Kuczera, K. *J. Chem. Phys.* **1997**, *107*, 8800.
(12) Phillips, L. A.; Webb, S. P.; Clark, J. H. *J. Chem. Phys.* **1985**, *83*, 5810.
(13) Kivelson, D.; Spears, K. G.; *J. Phys. Chem.* **1985**, *89*, 1999.
(14) Templeton, E. F. G.; Kenney-Wallace, G. A. *J. Phys. Chem.* **1986**, *90*, 2896.
(15) Templeton, E. F. G.; Kenney-Wallace, G. A. *J. Phys. Chem.* **1986**, *90*, 5441.
(16) Kenney-Wallace, G. A.; Paone, S.; Kalpouzos, C. *Faraday Discuss. Chem. Soc.* **1988**, *85*, 185.
(17) Simon, J. D.; Thompson, P. A. *J. Chem. Phys.* **1990**, *92*, 2891.
(18) Dutt, G. B.; Doraiswamy, S.; Periasamy, N.; Venkataraman, B. *J. Chem. Phys.* **1990**, *93*, 8498.
(19) Alavi, D. S.; Hartman, R. S.; Waldeck, D. H. *J. Chem. Phys.* **1991**, *94*, 4509.
(20) Alavi, D. S.; Hartman, R. S.; Waldeck, D. H. *J. Chem. Phys.* **1991**, *95*, 6770.
(21) Alavi, D. S.; Waldeck, D. H. *J. Phys. Chem.* **1991**, *95*, 4842.
(22) Hartman, R. S.; Alavi, D. S.; Waldeck, D. H. *J. Phys. Chem.* **1991**, *95*, 7872.
(23) Hartman, R. S.; Waldeck, D. H. *J. Phys. Chem.* **1994**, *98*, 1386.
(24) Hartman, R. S.; Konitsky, W. M.; Waldeck, D. H.; Chang, Y. J.; Castner, E. W., Jr. *J. Chem. Phys.* **1997**, *106*, 7920.
(25) Kurnikova, M. G.; Balabai, N.; Waldeck, D. H.; Coalson, R. D. *J. Am. Chem. Soc.* **1998**, *120*, 6121.
(26) Horng, M.-L.; Gadecki, J. A.; Maroncelli, M. *J. Phys. Chem. A* **1997**, *101*, 1030.
(27) Laitinen, E.; Korppi-Tommola, J and Linnanto, J. *J. Chem. Phys.* **1997**, *107*, 7601.
(28) Dutt, G. B.; Singh, M. K.; Sapre, A. V. *J. Chem. Phys.* **1998**, *109*, 5994.
(29) Dutt, G. B.; Raman, S. *J. Chem. Phys.* **2001**, *114*, 6702.
(30) Dutt, G. B.; Krishna, G. R.; Raman, S. *J. Chem. Phys.* **2001**, *115*, 4732.
(31) Dutt, G. B.; Ghanty, T. K.; Singh, M. K. *J. Chem. Phys.* **2001**, *115*, 10845.
(32) Dutt, G. B.; Ghanty, T. K. *J. Chem. Phys.* **2002**, *116*, 6687.
(33) Dutt, G. B.; Ghanty, T. K. *J. Chem. Phys.* **2003**, *118*, 4127.
(34) Wiemers, K.; Kauffman, J. F. *J. Phys. Chem. A* **2000**, *104*, 451.
(35) Spears, K. G.; Steinmetz, K. M. *J. Phys. Chem.* **1985**, *89*, 3623.
(36) Moog, R. S.; Bankert, D. L.; Maroncelli, M. *J. Phys. Chem.* **1993**, *97*, 1496.
(37) Dutt, G. B.; Srivatsavoy, V. J. P.; Sapre, A. V. *J. Chem. Phys.* **1999**, *110*, 9623.
(38) Dutt, G. B.; Srivatsavoy, V. J. P.; Sapre, A. V. *J. Chem. Phys.* **1999**, *111*, 9705.
(39) Dutt, G. B.; Krishna, G. R. *J. Chem. Phys.* **2000**, *112*, 4676.
(40) Dutt, G. B. *J. Chem. Phys.* **2000**, *113*, 11154.
(41) Hartman, R. S.; Konitsky, W. M.; Waldeck, D. H. *J. Am. Chem. Soc.* **1993**, *115*, 9692.
(42) Balabai, N.; Waldeck, D. H. *J. Phys. Chem. B* **1997**, *101*, 2339.
(43) Balabai, N.; Kurnikova, M. G.; Coalson, R. D.; Waldeck, D. H. *J. Am. Chem. Soc.* **1998**, *120*, 7944.
(44) Balabai, N.; Sukharevsky, A.; Read, I.; Strazisar, B.; Kurnikova, M.; Hartman, R. S.; Coalson, R. D.; Waldeck, D. H. *J. Mol. Liq.* **1998**, *77*, 37.
(45) O'Connor, D. V.; Phillips, D. *Time-Correlated Single Photon Counting*; Academic Press: London, 1984.
(46) Bevington, P. R. *Data Reduction and Error Analysis for the Physical Sciences*; McGraw-Hill: New York, 1969.
(47) Knutson, J. R.; Beechem, J. M.; Brand, L. *Chem. Phys. Lett.* **1983**, *102*, 501.
(48) Martin, D.; Hauthal, H. G. *Dimethyl Sulphoxide*; Halsted Press: New York, 1975.
(49) Schmidt, M. W.; Baldridge, K. K.; Boatz, J. A.; Elbert, S. T.; Gordon, M. S.; Jensen, J. H.; Koseki, K.; Matsunaga, N.; Nguyen, K. A.; Su, S.; Windus, T. L.; Dupuis, M.; Montgomery, J. A., Jr. *J. Comput. Chem.* **1993**, *14*, 1347.
(50) Drexhage, K. H.; Erikson, G. R.; Hawks, G. H.; Reynolds, G. A. *Opt. Commun.* **1975**, *15*, 399.
(51) Tominaga, K.; Walker, G. C. *J. Photochem. Photobiol. A: Chem.* **1995**, *87*, 127.
(52) Debye, P. *Polar Molecules*; Dover: New York, 1929.
(53) Perrin, F. *J. Phys. Radium* **1934**, *5*, 497.
(54) Edward, J. T. *J. Chem. Educ.* **1970**, *47*, 261.
(55) Sension, R. J.; Hochstrasser, R. M. *J. Chem. Phys.* **1993**, *98*, 2490.
(56) Small, E. W.; Isenberg, I. *Biopolymers* **1977**, *16*, 1907.
(57) Einstein, A *Investigations on the Theory of Brownian Movement*; Dover: New York, 1956.
(58) Gierer, A.; Wirtz, K. *Z. Naturforsch.* **1953**, *A8*, 532.
(59) Dote, J. L.; Kivelson, D.; Schwartz, R. N. *J. Phys. Chem.* **1981**, *85*, 2169.
(60) Nee, T. W.; Zwanzig, R. *J. Chem. Phys.* **1970**, *52*, 6353.
(61) van der Zwan, G.; Hynes, J. T. *J. Phys. Chem.* **1985**, *89*, 4181.
(62) Alavi, D. S.; Waldeck, D. H. *J. Chem. Phys.* **1991**, *94*, 6196.
(63) Alavi, D. S.; Waldeck, D. H. *J. Chem. Phys.* **1991**, *98*, 3580.
(64) Kurnikova, M. G.; Waldeck, D. H. Coalson, R. D. *J. Chem. Phys.* **1996**, *105*, 628.
(65) Kumar, P. V.; Maroncelli, M. *J. Chem. Phys.* **2000**, *112*, 5370.
(66) McWeeny, R. *Coulson's Valence*, 3rd ed.; Oxford University Press: London, 1979.
(67) Waldeck, D. H. *Conformational Analysis of Molecules in Excited States*; Waluk, J., Ed.; Wiley-VCH: New York, 2000; pp 113−176.
(68) Barthel, J.; Behert, H.; Schmithals, F. *Ber. Bunsen-Ges. Phys. Chem.* **1971**, *75*, 305.